Supporting Information

Designing High-Performance P3-type $Na_{2/3}[Ni_{1/3}Mn_{2/3}]O_2$ Cathodes for Na-ion Batteries

Changhee Lee,[a] Shun Nakajima,[a] Shinichi Kumakura,[a] Tomooki Hosaka,[a] Eun Jeong Kim[a] and Shinichi Komaba*[a]

[a]Department of Applied Chemistry, Tokyo University of Science, Shinjuku, Tokyo 162-8601, Japan.

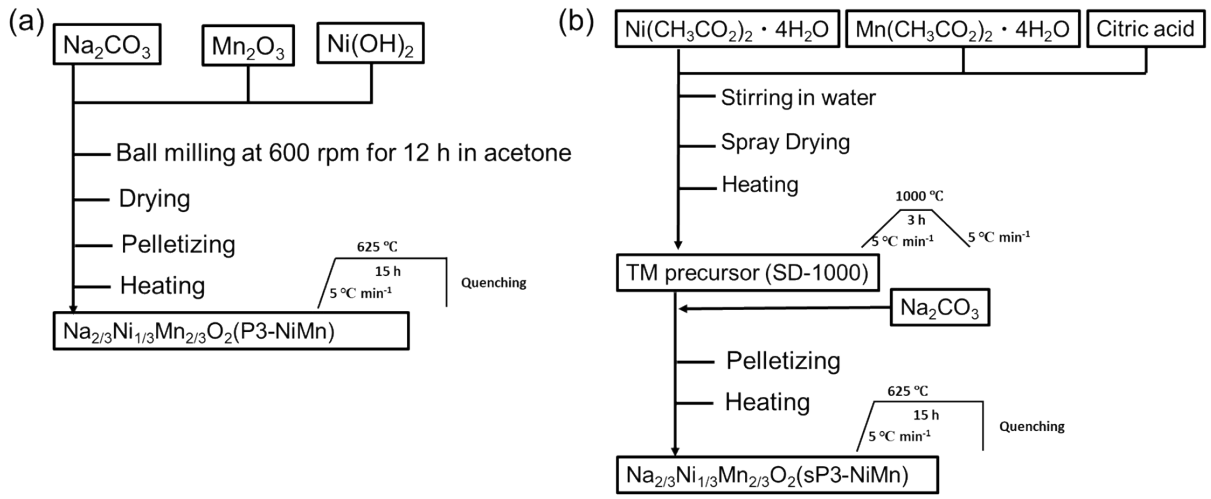

Figure S1. Synthesis process of (a) a one-step conventional P3-NiMn and (b) two-step spinel-derived P3-NiMn.

Table S1. Summary of the FWHM of the 131 XRD peak and the a-axis lattice parameter of the synthesized spinel $NiMn_2O_4$ precursors corresponding to **Figure 1c.**

Sample	FWHM of 131 peak / deg.	Lattice parameter of a (=b, c) / Å
SD-1000	0.0661	8.3971(8)
SD-1100	0.1096	8.4035(3)
SD-1200	0.0684	8.4023(5)
BM-1000	0.0757	8.4019(3)

Table S2. Rietveld refinement results on a synchrotron XRD pattern of SD-1000.

Space group *Fd*-3*m*						
a = 8.39158(2)Å, V = 590.9228(21) Å^3 R_{wp} = 9.810 %, R_B = 2.801%, R_F = 3.430%, S = 5.304						
Atom	Site	x	y	z	Occ.	B / Å^2
Ni1	8b	0.375	0.375	0.375	0.0228(53)	0.5*
Mn1	8b	0.375	0.375	0.375	0.9772(53)	0.5*
Ni2	16c	0.000	0.000	0.000	0.4886(53)	0.5*
Mn2	16c	0.000	0.000	0.000	0.5114(53)	0.5*
O1	32e	0.23686(8)	0.23686(8)	0.23686(8)	1.0*	0.7*

The Rietveld refinement results exhibit the crystal structure of spinel-type $NiMn_2O_4$, in which Mn^{2+} occupies the tetrahedral (8b) sites, while the octahedral (16c) sites are shared by Ni^{3+} and Mn^{3+} in a 1:1 ratio, corresponding to inverse spinel configuration.

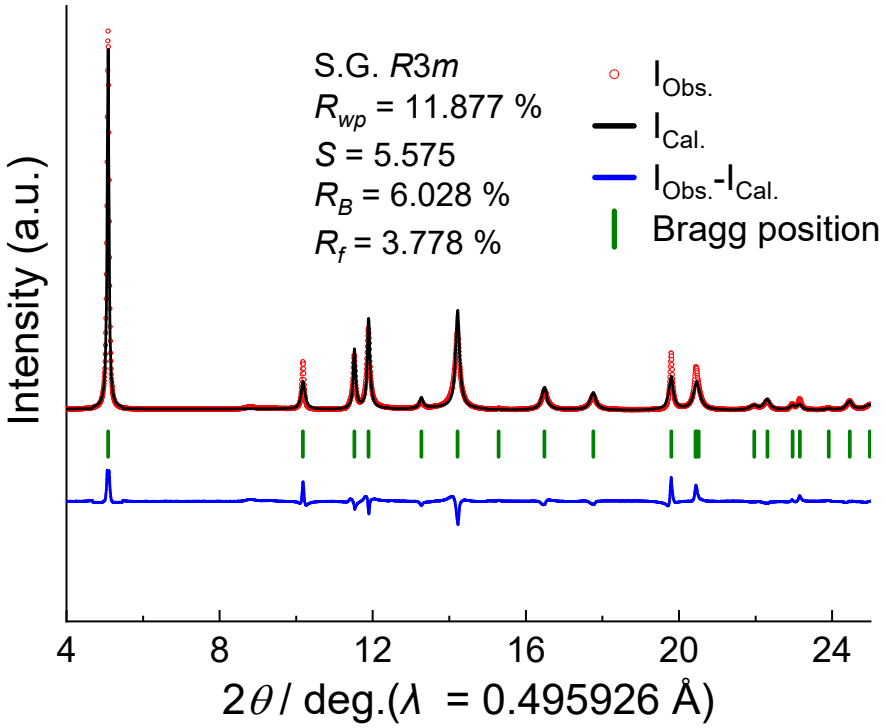

Figure S2. Rietveld refinement results on a synchrotron XRD pattern of cP3-NiMn.

Table S3. Rietveld refinement results on a synchrotron XRD pattern of cP3-NiMn.

Space group R3m						
a = 2.88306(15) Å, c = 16.76626(103) Å, V = 120.6908 (114) Å^3						
Atom	Site	x	y	z	Occ.	B / Å^2
Na	3a	0	0	0.16889(24)	0.667*	1.0*
Ni	3a	0	0	0	0.333*	0.5*
Mn	3a	0	0	0	0.667*	0.5*
O1	3a	0	0	0.39324(64)	1.0*	0.7*
O2	3a	0	0	-0.39104(61)	1.0*	0.7*

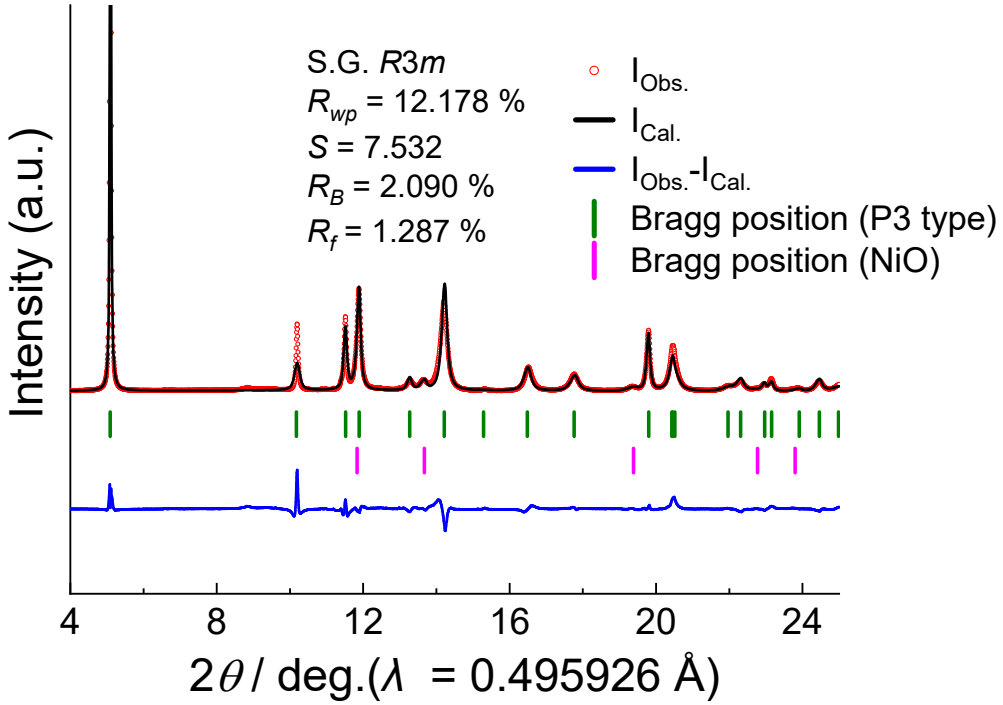

Figure S3. Rietveld refinement results on a synchrotron XRD pattern of sP3-NiMn.

Space group R3m						
a = 2.88502(15) Å, c = 16.73549(103) Å, V = 120.6328 (117) Å^3						
Atom	Site	x	y	z	Occ.	B / Å^2
Na	3a	0	0	0.17095(28)	0.667*	1.0*
Ni	3a	0	0	0	0.333*	0.5*
Mn	3a	0	0	0	0.667*	0.5*
O1	3a	0	0	0.39422(76)	1.0*	0.7*
O2	3a	0	0	-0.39342(74)	1.0*	0.7*

Table S4. Rietveld refinement results on a synchrotron XRD pattern of sP3-NiMn.

P3 : NiO = 97.0 : 3.0 (wt%)

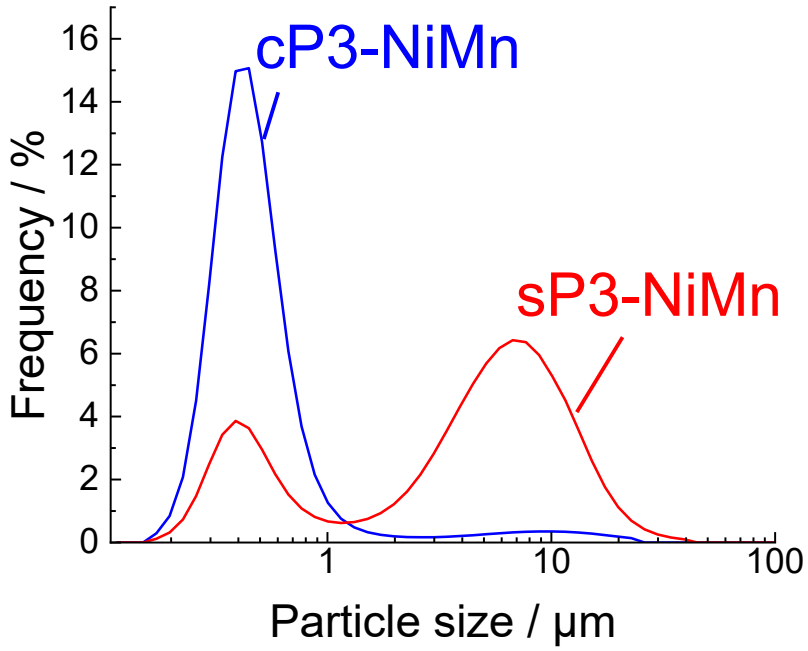

Figure S4. Particle size distribution of cP3-NiMn and sP3-NiMn powders.

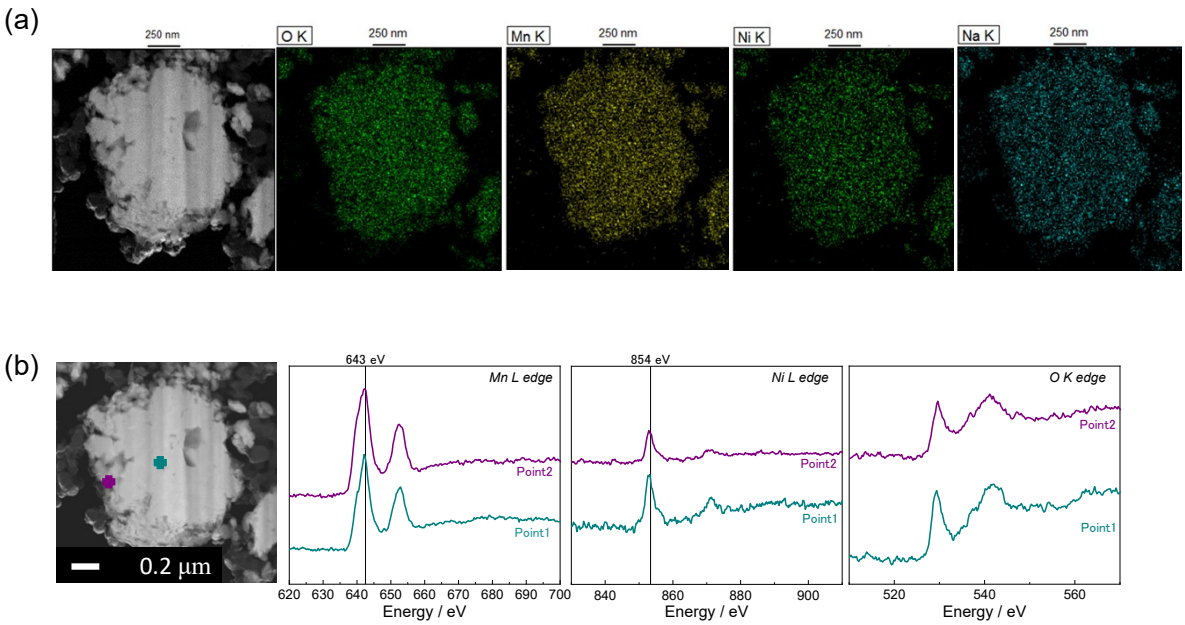

Figure S5. (a) STEM and EDS mapping images and (b) EELS spectra of Mn L, Ni L, and O K-edges of cP3-NiMn.

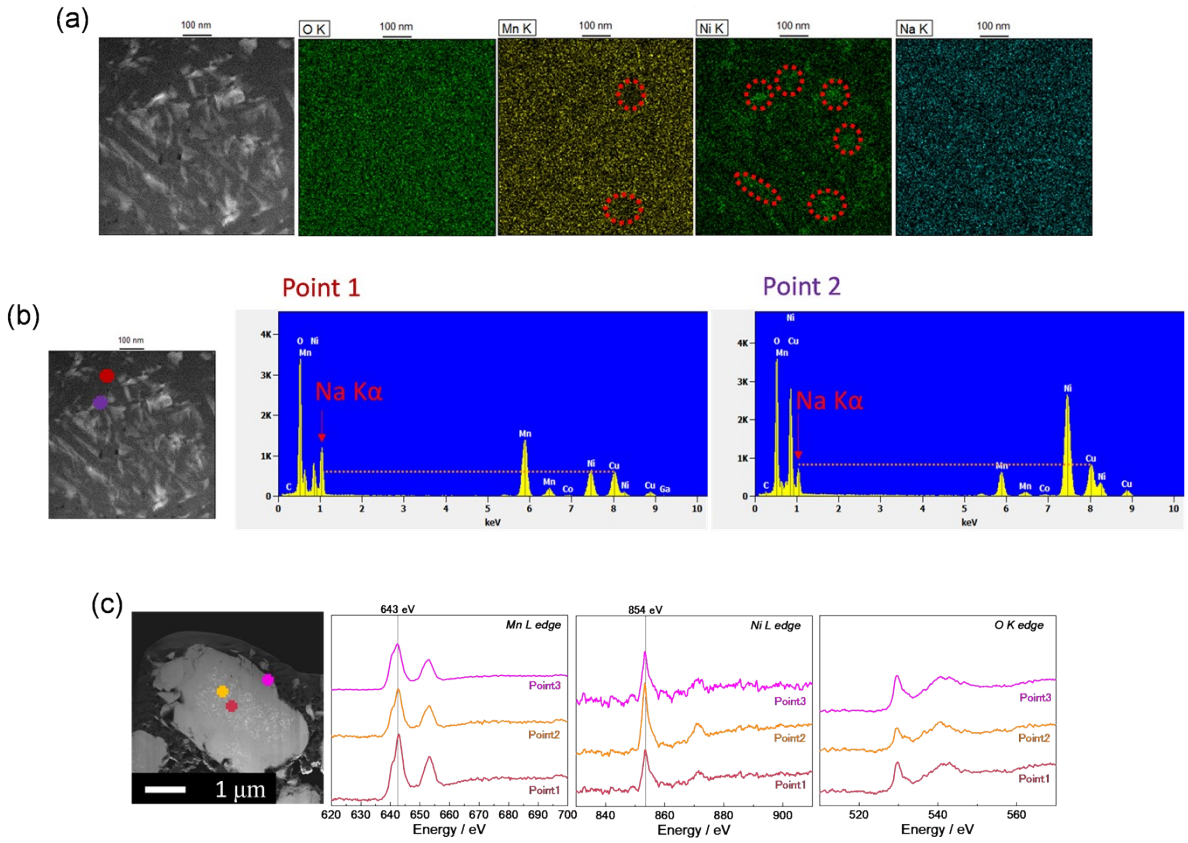

Figure S6. (a) STEM and EDS mapping images, (b) EDS spectra, and (c) EELS spectra of Mn L, Ni L, and O K-edges of sP3-NiMn.

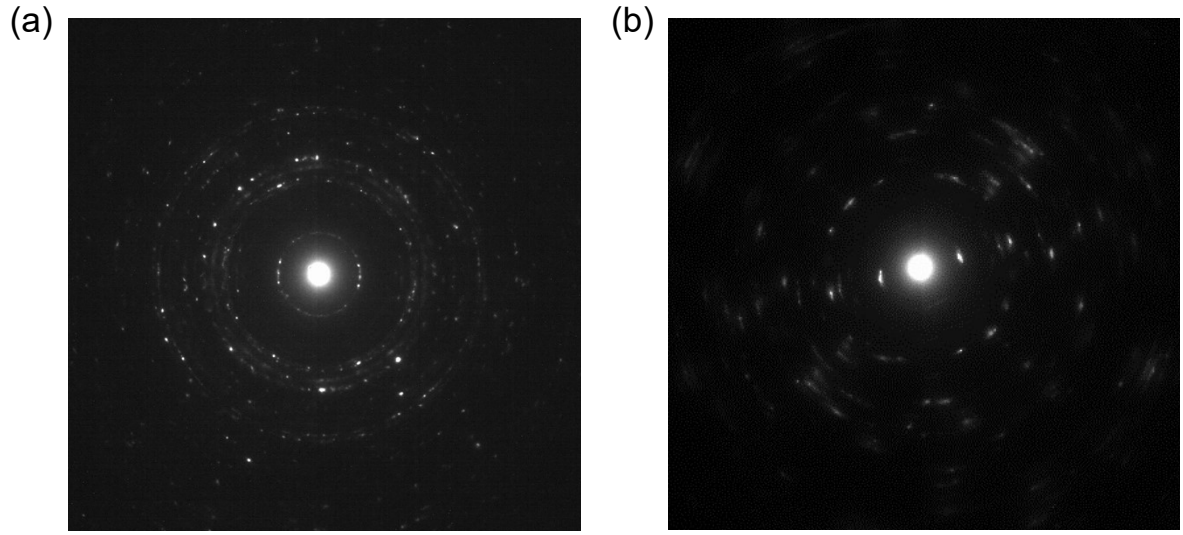

Figure S7. Selected area electron diffraction (SAED) patterns corresponding to the STEM images of (a) cP3-NiMn and (b) sP3-NiMn.

The observed SAED patterns confirm the polycrystalline nature of both cP3-NiMn and sP3-NiMn.

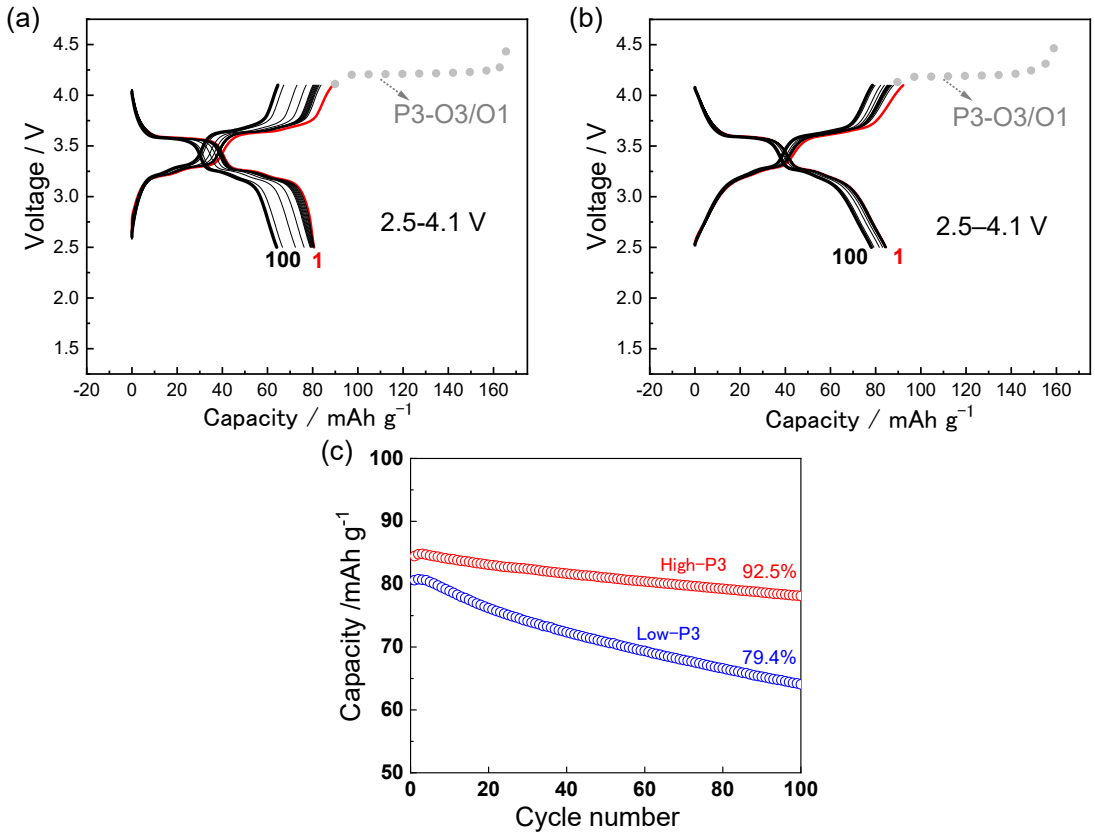

Figure S8. Charge/discharge curves of (a) cP3-NiMn and (b) sP3-NiMn in 1 mol dm^{-3} $NaPF_6$/PC with 2 vol% FEC at C/10 (1C = 260 mA g^{-1}) within volage ranges of 2.5–4.1 V (vs Na). (c) Cycle performance comparison of cP3-NiMn and sP3-NiMn in 1 mol dm^{-3} $NaPF_6$/PC with 2 vol% FEC at C/10 (1C = 260 mA g^{-1}) within volage ranges of 2.5–4.1 V (vs Na).

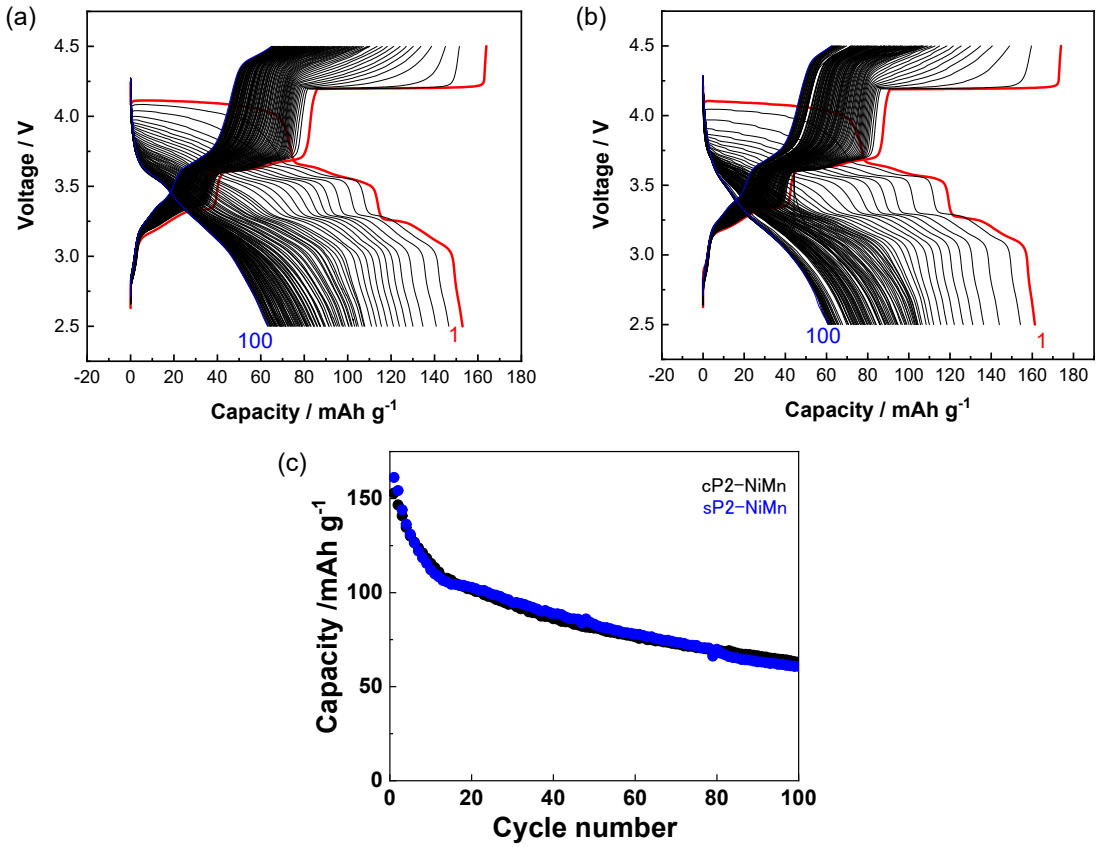

Figure S9. Charge/discharge curves of (a) cP2-NiMn and (b) sP2-NiMn in 1 mol dm^{-3} $NaPF_6$/PC with 2 vol% FEC at C/10 (1C = 260 mA g^{-1}) within volage ranges of 2.5–4.5 V (vs Na). (c) Cycle performance comparison of cP3-NiMn and sP3-NiMn in 1 mol dm^{-3} $NaPF_6$/PC with 2 vol% FEC at C/10 (1C = 260 mA g^{-1}) within volage ranges of 2.5–4.5 V (vs Na).

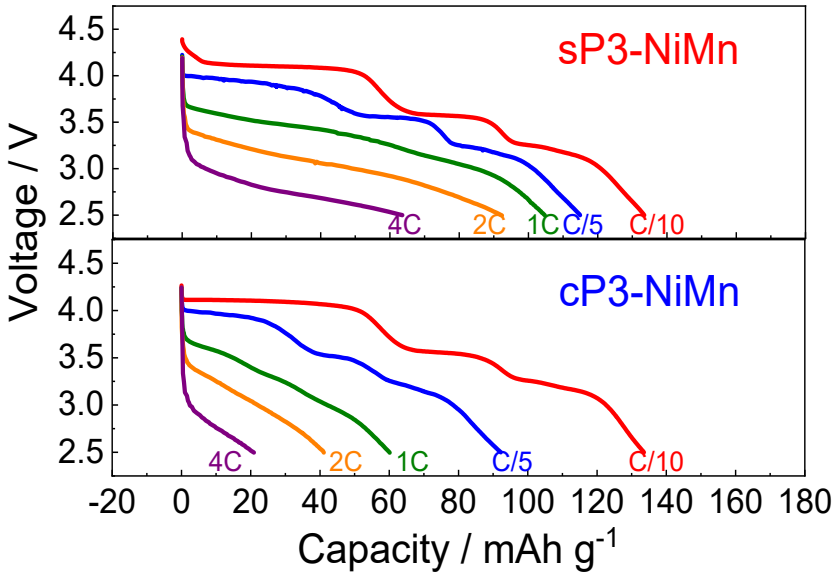

Figure S10. Discharge curves of sP3-NiMn and cP3-NiMn with different rates, corresponding to **Figure 2h**.

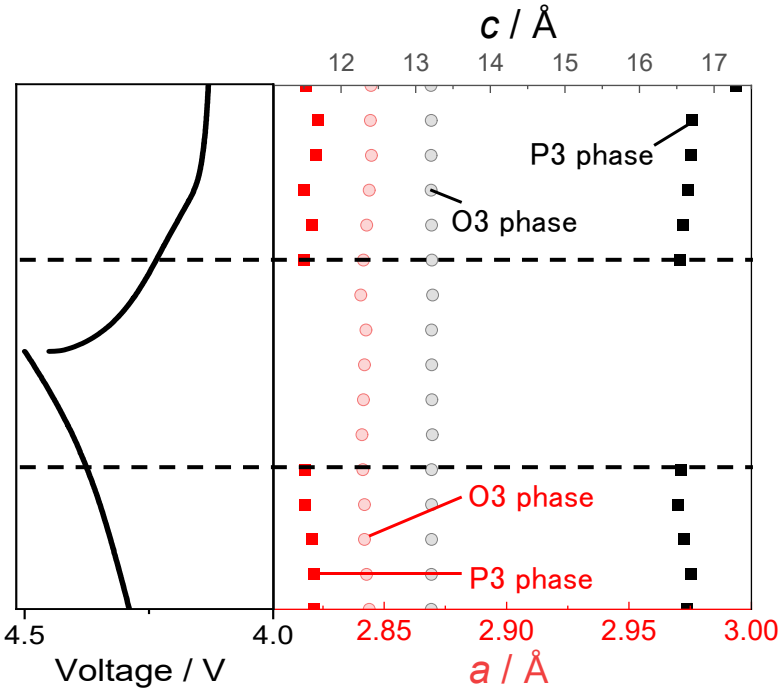

Figure S11. A magnified view of **Figure 4b**

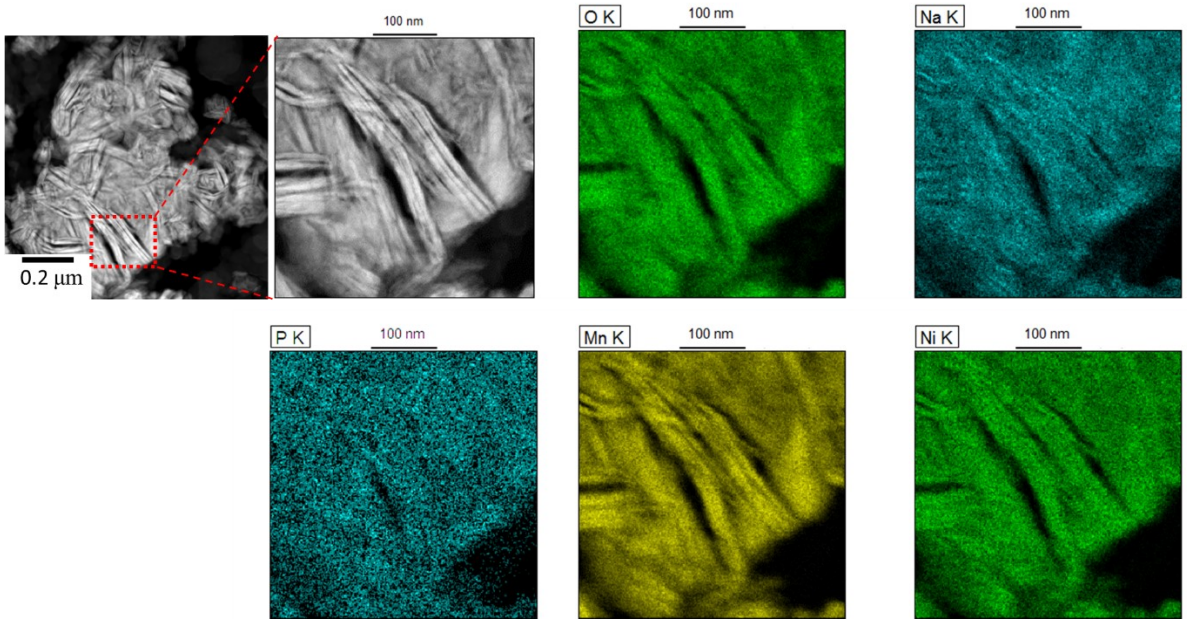

Figure S12. STEM and EDS mapping images of cP3-NiMn after 100 cycles.

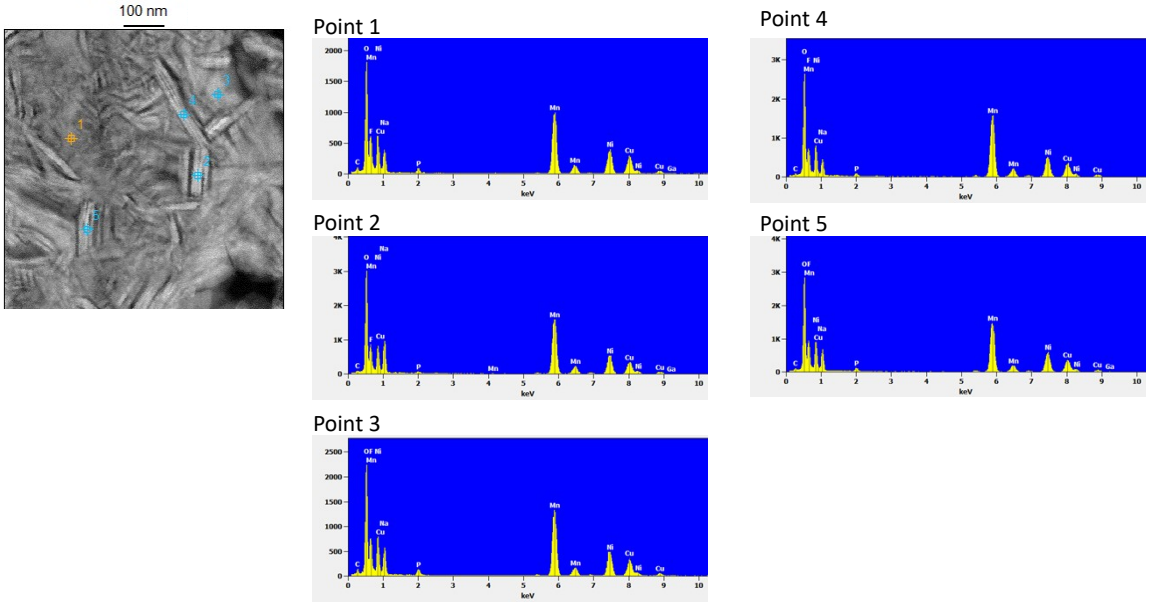

Figure S13. STEM and EDS spectra of cP3-NiMn after 100 cycles.

Cracks were observed throughout the material, occurring in both surface and bulk regions.

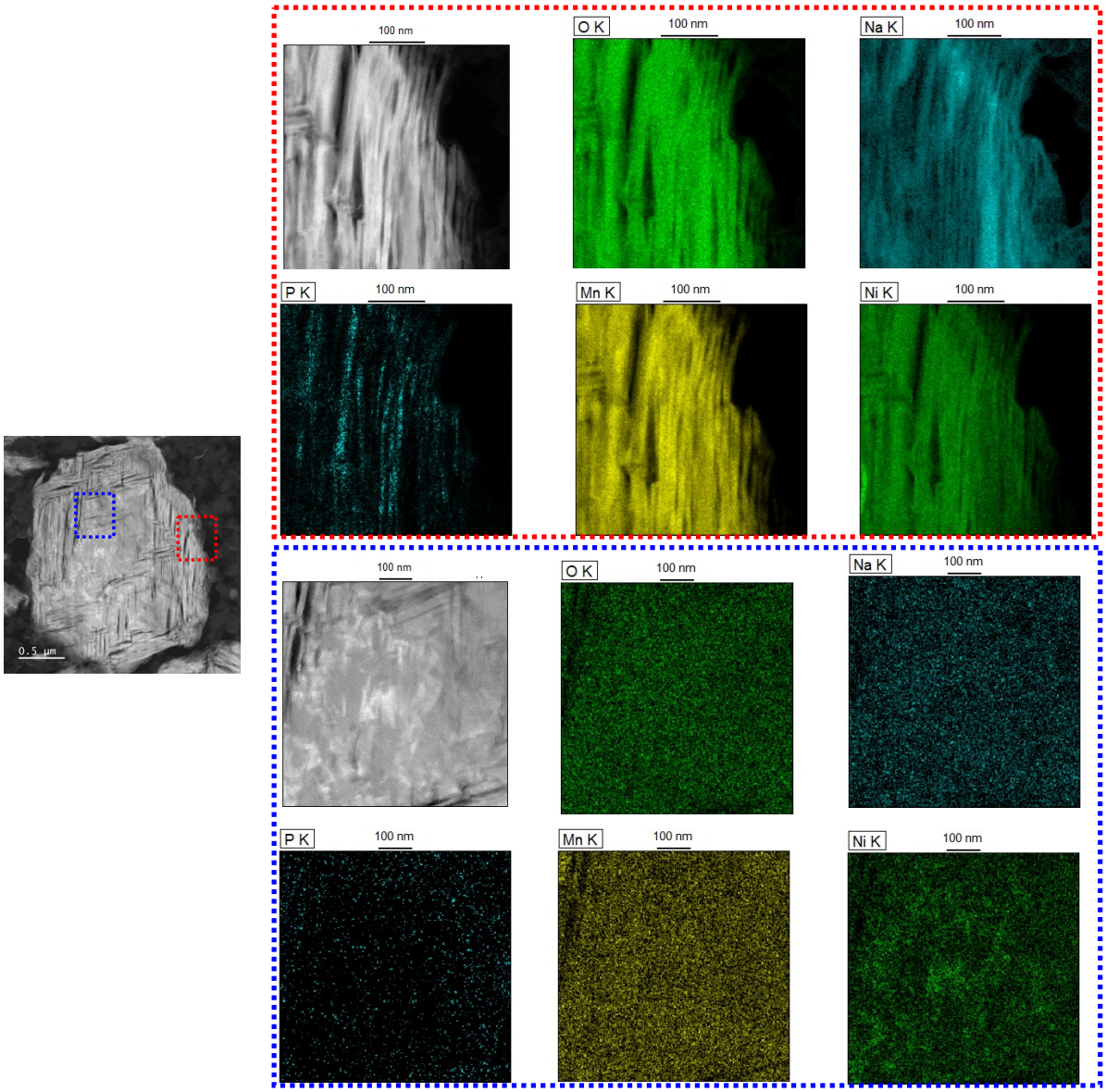

Figure S14. STEM and EDS mapping images of sP3-NiMn after 100 cycles.

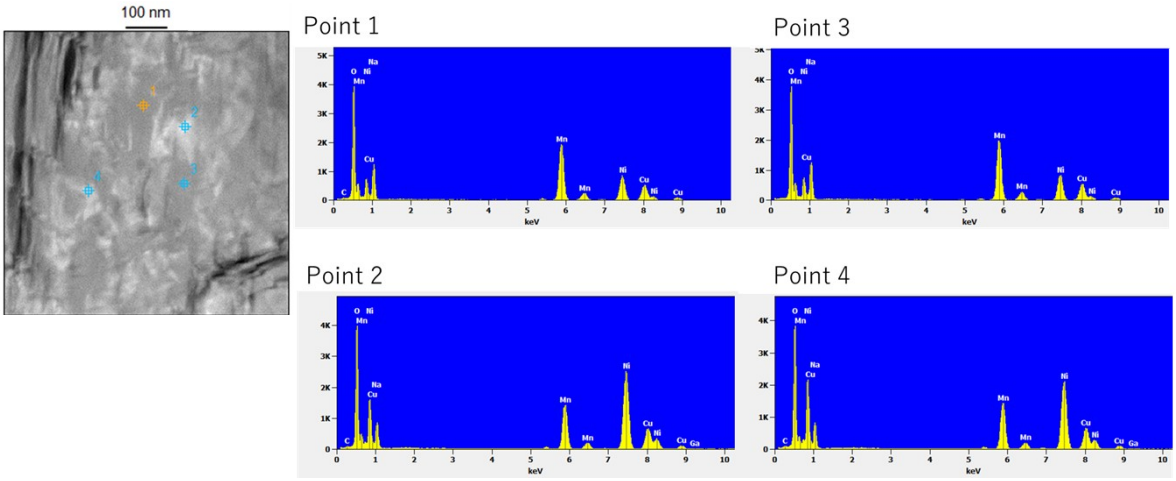

Figure S15. STEM and EDS spectra of sP3-NiMn after 100 cycles.

The Ni-rich region (NiO) was found to remain structurally intact without significant degradation.

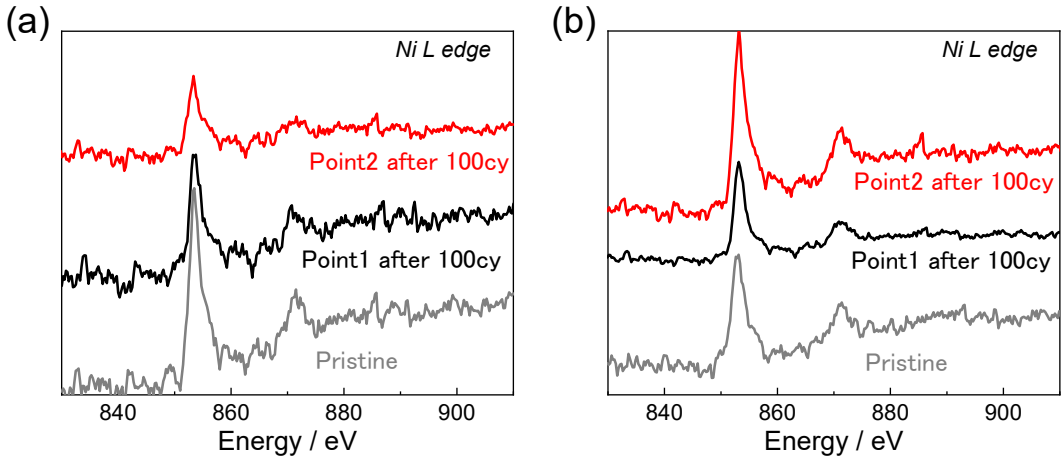

Figure S16. EELS spectra of Ni L edge of (a) cP3-NiMn and (b) sP3-NiMn.

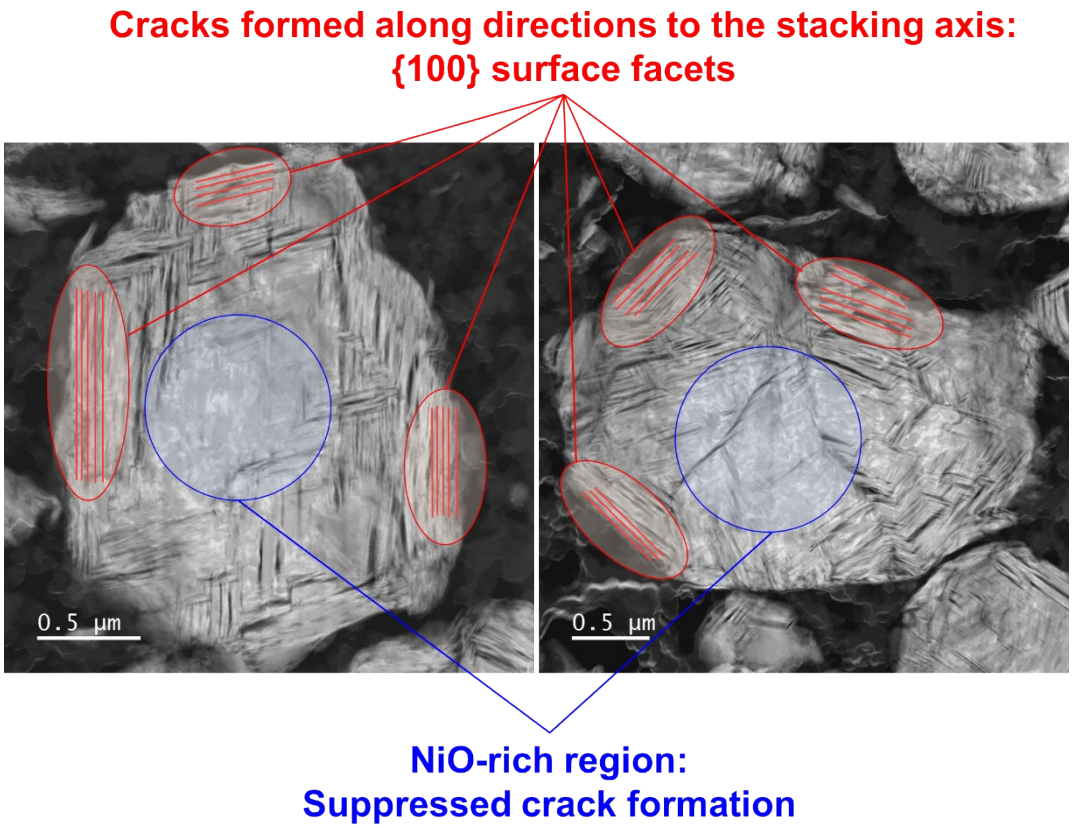

Figure S17. STEM images of two individual sP3-NiMn particles obtained under the same conditions after 100 cycles, showing NiO-rich regions and exposed {100} surface facets associated with the presence of cracks.